DESY Summer Student Program 2009
Report No.

Characterization of Silicon Photomultipliers and their Application to Positron Emission Tomography

Zhiwei Yang

V. N. Karazin Kharkiv National University

E-mail: Prince4563@yahoo.com

Abstract

As a summer student at DESY in 2009, I joined the FLC group (Forschung mit Lepton Collidern) which is involved in the International Linear Collider project. My task was to verify the feasibility of silicon photomultipliers in PET applications using an experimental setup built at DESY. Having little experience in this subject, I had to acquire some basic knowledge on Linux operating system , C++ programming language, ROOT analysis program and editing programs, on electronics devices and photodetectors, to perform the needed measurements.

I. Introduction

In the past decade silicon photomultipliers (SiPM) have been increasingly used in several kind of applications in physics. Their typical signal amplification is now comparable to the signal gain observed in standard photomultiplier tubes. The silicon technology permits also the production of small devices (millimeter scale), thus allowing their use in highly granulated and segmented calorimeters for high energy physics. Some detector concepts for the foreseen International Linear Collider (ILC) [1] are based on SiPMs for signal readout.

As detector counters, SiPMs can be used also in medical imaging applications as in PETs. The subject of this work is to show the feasibility to use SiPMs in PETs using an experimental setup built at DESY to precisely identify (via SiPMs) back-to-back photons emitted by a radiative source..

The report has the following structure. The devices used in this work are introduced in sections 2~4. The measurements for characterizing silicon photomultipliers are presented in section 5. The eventual application of SiPMs in a PET-like setup is the subject of section 6.

2. Characteristics of Silicon Photomultipliers

Silicon photomultipliers [2]-[3] are photon sensitive devices built from an avalanche photodiode (APD) array on a common Si substrate. The idea behind this device is the detection of single photon events in sequentially connected silicon APDs. The dimension of each single APD can vary from 20 to 100 micrometers, and their density can be up to 1000 per millimeter square. Every APD in a SiPM is operated in Geiger mode and is coupled with the others by a polysilicon quenching resistor. When an incident photon generates an electron-hole pair in the p-n junction, then an avalanche of electrons can be created by the sufficiently high electric field driving the primary electron through the junction. The detection of a photon thus appears as a current pulse at the APD cathode. The signal output from the entire SiPM device is the total sum of the outputs from the individual APD pixels. Although the device works in digital switching mode, the SiPM is an analog device because all the microcells are read in parallel making possible to generate signals within a dynamic range from one single photon to 1000 photons for a device of just a single square millimeter area. The supply voltage depends on the used APD technology, and typically varies between 25 V and 70 V, thus being from 30 to 50 times lower than the voltage required for a traditional photomultiplier tubes (PMTs) operation. Due to the limited number of pixels and to the finite pixel recovery time (50~100 ns) silicon photomultipliers are typically non-linear devices due to saturation. SiPMs offer the high-performance needed in photon counting and are used in diverse applications for detecting extremely weak light at the photon counting level. SiPMs have been invented in Russia at Moscow Engineering Physics Institute. This design idea was then used with some variations by SensL, Photonique, Hamamatsu, Voxtel Inc., STMicroelectronics and other companies.

Typical specifications for a SiPM are:

1. Total quantum efficiency of about 20%, being similar to a traditional PMT;
2. Gain (G) similar to a PMT, being approximately 10^6;
3. The gain dependence on the applied voltage is linear, and does not follow a power law like in the case of PMTs;

4. Timing jitter optimized to have a photon arrival time resolution of about 100 ps;
5. Signal decay time inversely proportional to the square root of photoelectrons number within an excitation event;
6. The signal parameters are practically independent on external magnetic fields, contrary to what is observed with PMTs;
7. Small dimensions permit extremely compact, light and robust mechanical design.

In this work, SiPMs from the Center of Perspective Technology and Apparatus (CPTA), from Hamamatsu Photonics and Zecotek Photonics have been investigated. Typically, Hamamatsu SiPMs are known as Multi-Pixel Photon Counters (MPPC), while Zecotek devices are known as Micro-pixel Avalanche Photo Diodes (MAPD). The devices used here are:

1. CPTA SiPM**,** made of 556 pixels of size 43 μm, for a total dimension of approximately a circle of 1.12 mm. This device is available in the laboratory coupled to a 3×3 cm^2 scintillating tile via a wavelength shifter KURARAY Y11 (green light output) resulting in a photon detection efficiency at chosen voltage ~15%. The dark rate is 0.6-1.0 MHz and the gain around (0.5 -1.0) × 10^6;
2. HAMAMATSU MPPC-11-050M, of size1×1 mm^2, made of 400 pixels;
3. HAMAMATSU MPPC-33-050C, of size 3×3 mm^2, made of 3600 pixels;
4. Zecotek MAPD-3N, with 40000 pixels per mm^2.

3. Scintillating Materials

A scintillator [4] is a material which exhibits the property of luminescence when is excited by ionizing radiation. Luminescent materials, when struck by an incoming particle (ionizing radiation), absorb its energy and scintillate, i.e. re-emit the absorbed energy in the form of a small flash of light, typically in the visible range. If the re-emission occurs promptly, i.e. within the ~10^{-8}s required for an atomic transition, the process is called fluorescence.

A scintillation detector or scintillation counter is obtained when a scintillator is coupled to an electronic light sensor such as a photomultiplier tube (PMT) or a silicon photodiode. PMTs absorb the light emitted by the scintillator and re-emit it in the form of electrons via the photoelectric effect. The subsequent multiplication of those electrons (sometimes called photo-electrons) results in an electrical pulse which can then be analyzed and yield information about the particle that originally struck the scintillator. Silicon photodiodes accomplish the same thing directly in the silicon, as described in Sec. 2.

Among the properties desirable in a good scintillator are: a high light output (i.e. a high efficiency for converting the energy of incident radiation into scintillation photons), transparency to its own scintillation light (for good light collection), efficient detection of the radiation being studied, good linearity over a wide range of energy, a short rise time for fast timing applications (e.g. coincidence measurements), a short decay time to reduce detector dead-time and accommodate high event rates, emission in a spectral range matching the spectral sensitivity of existing photomultipliers.

The light output is the most important figure of merit of a scintillator, as it affects both the efficiency and the energy resolution of the detector. The efficiency is the ratio of detected particles to the total number of particles impinging upon the detector. The energy resolution is the ratio of the full width at half maximum of a given energy peak to the peak position, usually expressed in percent. The light output is a strong function of the type of incident particle and of its energy, which therefore strongly influences the type of scintillation material to be used in a particular application. The presence of quenching effects results in reduced light output (i.e. reduced scintillation efficiency). Quenching refers to all radiationless de-excitation processes in which the excitation is degraded mainly to heat. The overall signal production efficiency of the detector, however, also depends on the quantum efficiency of the photomultiplier, and on the efficiency of light transmission and collection (which depends on the type of reflector material covering the scintillator and light guides, on the length and shape of the light guides, on any light absorption, etc). The light output is often quantified as a number of scintillation photons produced per keV of deposited energy. For an incident electron, typical numbers are approximately 40, 10, and 4 photons per keV for NaI(TI), plastic scintillators, and BGO crystal, respectively.

The detection efficiency for electrons is essentially 100% for most scintillators. But, because electrons can make large angle scatterings, they can exit the detector without depositing their full energy in it. This scattering is a rapidly increasing function of the atomic number Z of the scintillator material. Organic scintillators, having a lower Z than inorganic crystals, are therefore best suited for the detection of low-energy (smaller than 10 MeV) electrons. The situation is different for high energy electrons. Since they mostly lose their energy by bremsstrahlung radiation at the higher energies, a higher-Z material is better suited for the detection of the bremsstrahlung photon and the production of the electromagnetic shower which it can induce.

High-Z materials, e.g. inorganic crystals, are best suited for the detection of gamma rays (E_γ larger than 100 keV). The photons interact with matter mainly via the photoelectric effect, pair production, and Compton scattering. In the photoelectric effect and pair production the photon is completely absorbed, while only partial energy is deposited in the Compton scattering. The cross section for the photoelectric process and pair production is proportional to Z^5 and Z^2, respectively, whereas Compton scattering depends roughly linearly on Z. A high-Z material therefore favors the former two processes, enabling the detection of the full energy of the gamma ray.

4. Positron Emission Tomography

Positron emission tomography (PET) [5] is a nuclear medicine imaging technique which produces a three-dimensional image of processes in the human body. The basis of PET is that a radionuclide (tracer) is introduced in the body via a biologically active molecule (called radiofarmaceutical). The molecule is optimized for a better uptake and retention by tissues of interest via metabolic process. thus localizing the tracer in the selected area of the body. Typically the FDG, made of deoxyglucose, is used, and the metabolic process is that of glucose utilization.

As the radioisotope undergoes positron emission decay, emitting a positron which loses energy through interactions with an electron in the surrounding tissue until it annihilates after traveling up to a few

millimeters into two photons moving in opposite directions. Each photon can be detected when they reach a scintillator in a scanning device (located around the tissues of interest), creating scintillating light which is detected by a photomultiplier vacuum tube or a silicon photomultiplier. The technique depends on coincident detection of the two photons moving in approximately opposite direction (it would be exactly opposite in their center of mass frame). Events with two photons which are not detected in coincidence within a narrow time window (a few nanoseconds) are rejected.

Detecting two collinear photons allows to localise the decay source (and to map the investigated tissue) within the spatial precision driven mainly by both the positron surviving distance before annihilation (below 2 mm) and by the size and design of the PET detector. Using traditional PMTs for readout results typically in the spatial resolution being dominated by the instrumentation. The recent introduction of small size SiPMs (1x1 mm^2) as readout component of the detector should instead allow to decrease the resolution down to the spatial uncertainty of the underlying physics process (decay plus annihilation).

An additional source of uncertainty for the tissue mapping is given by detecting background contributions to the measured events. One photon can experience Compton scattering with the tissue before being detected, thus biasing the reconstructed source location. It is crucial therefore to proper disentangle its contribution to the energy spectrum of the measured events. Compton photons should have lower energy than the photons immediately detected after positron-electron annihilation. Random coincidence, i.e. the detection within the same time window of two photons from two different uncorrelated annihilations, is also a source of background by erroneously assigning the event to a single positron emission. This background contribution, increasing linearly with the width of the coincidence time window, can be decreased properly reducing the time window width.

5. Measurements of SiPM Properties

In this section the properties of the measured SiPMs are presented. Although only one specific SiPM type was eventually used in the PET-like experiment, here the measurements done for several devices are shown for comparison. The signals from SiPMs are processed by ADC and QDC Modules. Therefore, to avoid biases to the data from possible non-linearity effects, the linearity of those modules was checked first.

5.1 Linearity of ADC and QDC Modules

An analog to digital converter (ADC) is a device which converts continuous signals to discrete digital numbers. It is used typically to measure the amplitude of a voltage pulse. A charge to digital converter (QDC) is used instead to measure the charge value of an electric pulse. The term linearity, as used here, means that the measured output values are in a linear relation with the input signal values.

The linearity of the modules LeCroy 1182 ADC & CAEN V965A QDC, used in this work, has been investigated. The experimental setup used in these measurements is presented in Fig. 1.

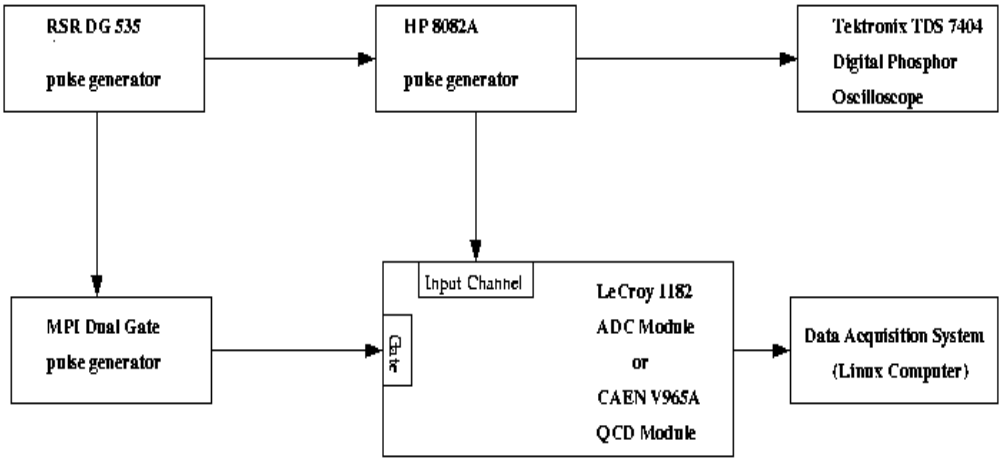

Fig. 1: Experimental setup used for the linearity measurement of the ADC and QDC modules.

A primary pulse generator (RSR DG 535) is used to originate two synchronized triggers. One signal triggers the second generator (HP 8082A) to send a squared voltage pulse to the ADC/QDC module. The second trigger is sent to a gate generator, which produces a pulse to open the ADC/QDC gate long enough to process the voltage pulse from the secondary generator. The ADC/QDC readout is then transferred to a Linux PC via the DAQ system and saved into ROOT files. To measure the signal amplitude an oscilloscope was used. The amplitude was varied in steps, and the corresponding ADC value was recorded. For each measurement step, the charge Q_{inj} injected to the ADC module was calculated according to the formula:

$$Q_{inj} = A_{inj} / \mathrm{R} \times W_{inj} .$$

In the formula A_{inj} and W_{inj} represent the amplitude and the width of the input voltage pulse, respectively, and R is the impedance of the line. The pedestal amplitude was measured by shifting the input signal out of ADC/QCD gate.

The result of the measurements for the two modules is presented in Tables 1-2, and shown in Fig. 2-3. In these pictures, the result of a linear fit is super imposed to the experimental data. The response of the two modules appear to be linear. For the LeCroy 1182 and CAEN V965A modules, when plotting the input charge values with respect to the measured one obtains from the linear fit 26.1 ± 0.4 and 225 ± 1 fC per ADC unit, respectively, reasonably in agreement with the values provided in the reference manual provided by the manufacturer (25 and 200 fC per ADC count).

INPUT				OUTPUT			
Amplitude [mV]	**Width [ns]**	**Resistance [Ω]**	**Charge [pC]**	**Signal [ADC]**	**Signal RMS**	**Pedestal [ADC]**	**ADC − Pedestal**
252	6.1	50	30.7	1080	10.7	340.6	739
332	6.1	50	40.5	1401	24.5	340.6	1060
378	6.1	50	46.1	1605	29.1	307.0	1298
451	6.1	50	55.0	1922	30.9	340.6	1581
497	6.1	50	60.6	2134	32.1	311.0	1823
548	6.1	50	66.9	2377	34.4	318.0	2059
613	6.1	50	74.8	2722	34.2	320.0	2402
672	6.1	50	82.0	2974	42.5	318.0	2656
737	6.1	50	89.9	3272	31.7	314.0	2958
789	6.1	50	96.3	3550	30.5	309.0	3241

Table 1: Measurement of the linearity response for the LeCroy 1182 ADC module.

INPUT				OUTPUT			
Amplitude [V]	**Width [ns]**	**Resistence [Ω]**	**Charge [pC]**	**Signal [ADC]**	**Signal RMS**	**Pedestal [ADC]**	**ADC - Pedestal**
0.13	22	50	57.2	176	1.1	62	114
0.35	22	50	154.0	602	2.2	62	540
0.55	22	50	242.0	988	2.6	62	926
0.80	22	50	352.0	1472	3.9	62	1410
1.07	22	50	470.8	1992	3.7	62	1930
1.28	22	50	563.2	2403	4.1	62	2341
1.43	22	50	629.2	2694	4.2	62	2632
1.59	22	50	699.6	3010	3.8	62	2948
1.77	22	50	778.8	3358	3.9	62	3296
2.00	22	50	880.0	3797	3.7	62	3735

Table 2: Measurement of the linearity response for the CAEN V965A module.

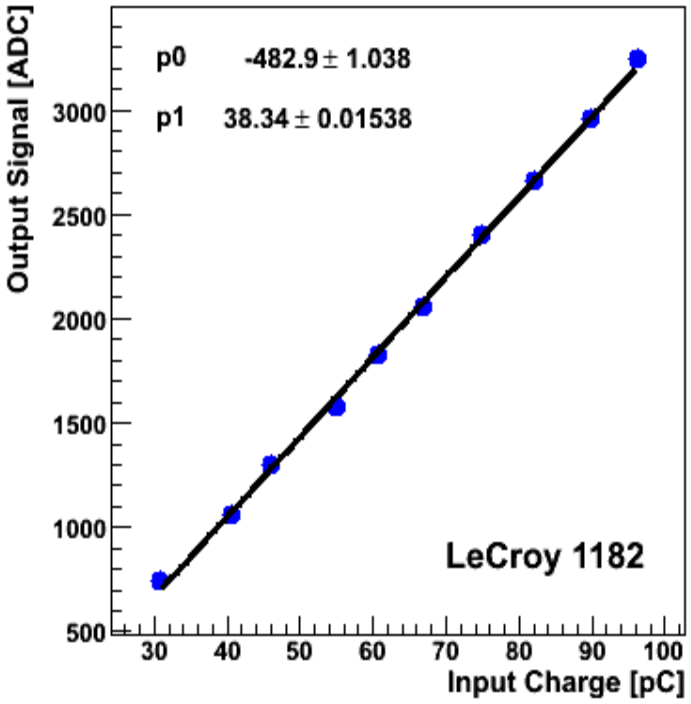

Fig. 2.: Dependence of LeCroy 1182 module response on the charge of the input signal.

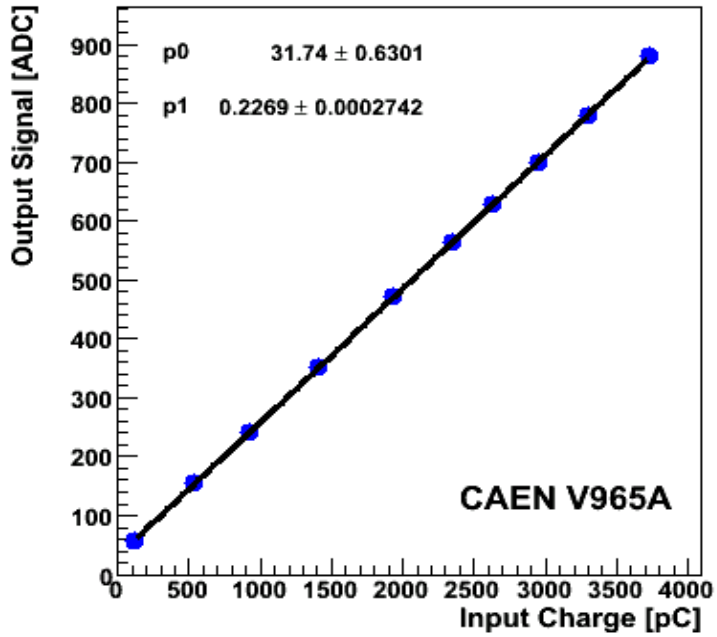

Fig. 3.: Dependence of CAEN V965A response on the charge of input signal.

5.2 CPTA Silicon Photomultipliers

The experimental setup used in these measurements is shown in Fig. 4. For the readout, the CAEN V965A was here used, with the gate width of 70 ns. The photodetector is coupled to a scintillating plate via a wavelength shifter.

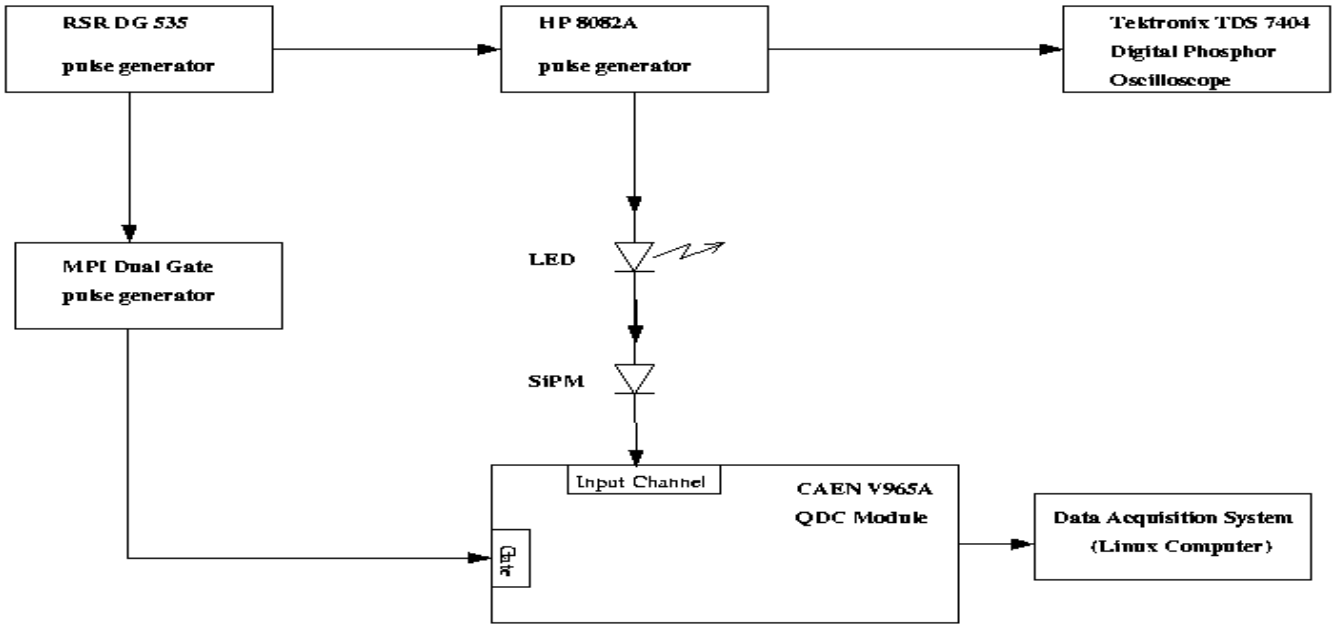

Fig. 4.: Experimental setup for the measurement of linearity of Silicon Photomultipliers. In case of MPPCs and CPTA SiPMs a 5X, 20X or 50X amplifier was located between the photomultiplier and the input channel of the ADC module.

The use of an amplifier (5X) between the SiPM and the ADC allows to distinguish the contribution of the single pixels to the SiPM spectrum. The ADC values of the separated photo-electron peaks are presented in Tab. 3. The first peak corresponds to the pedestal. The second peak corresponds to one pixel firing, the third one to the two pixels firing, and so on. The peak amplitude values measured in ADC units can be then converted into number of firing pixels.

V_{SiPM} [V]	$S_{Amplifier}$	ADC_{pk2}	ADC_{pk3}	ADC_{pk4}	$ADC_{pk3} - ADC_{pk2}$	$ADC_{pk4} - ADC_{pk3}$	**ADC units per pixel**
-29	5	113	124	135	11	11	11 (5X) 2.2 (1X)

Table 3: Measurement of single-pixel position values (in ADC units) in the spectrum of CPTA SiPM with size 1×1 mm² and 556 pixels. Measuring the distance between two peaks in ADC values, the ADC units can be quantified into number of photo-electron peaks.

The response of the CPTA device with respect to different amplitude values of the input light has been measured by varying the output voltage of the secondary pulse generator HP 8082A. The measurement is shown in Fig. 5, and the values are presented in Tab. 4 in terms of numbers of effective firing pixels, calculated as described above. The expected non-linear behavior is visible in the measurement.

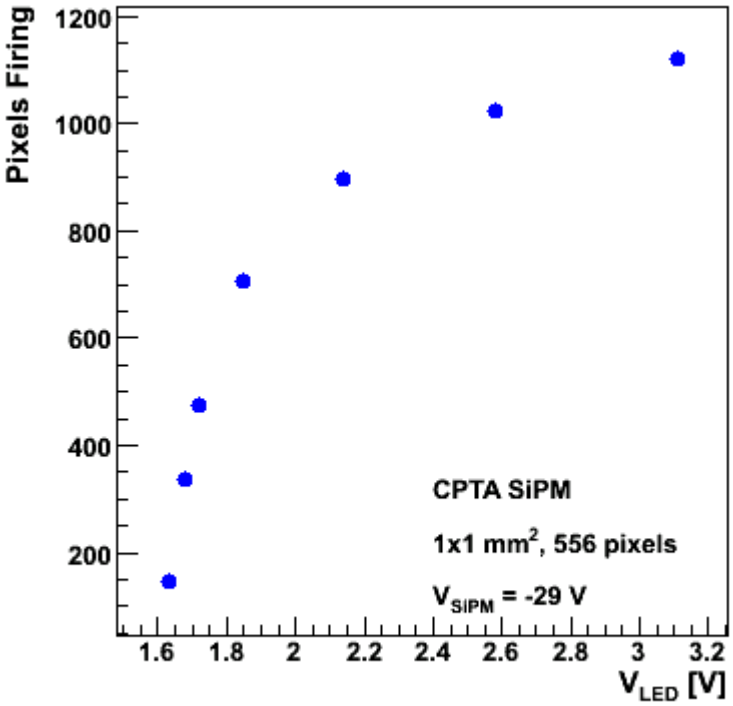

Fig. 5.: Response (in number of photo-electron pixels) of the CPTA SiPM on the input light intensity, presented in terms of the voltage value applied to the LED source.

INPUT	**OUTPUT**				
V_{LED} **[V]**	**Signal [ADC]**	**Signal RMS**	**Pedestal [ADC]**	**Signal - Pedestal**	**Nr. of Pixels**
1.63	420	28	100	320	144.3
1.68	845	31	100	745	335.8
1.72	1155	28	100	1055	475.4
1.85	1670	19	100	1570	707.4
2.14	2094	12	100	1994	898.4
2.58	2370	10	100	2270	1022.7
3.11	2584	10	100	2484	1119.1

Table 4: Measurement of the CPTA SiPM response to the input signal amplitude.

From the peak to peak distance (in ADC units) the gain of the CPTA device can be calculated using the ADC to charge conversion factor M_{ADC} according to the formula

$$G_{SiPM} = (ADC_{pk-pk} / S_{Amplifier}) \times M_{ADC} / e .$$

In the formula, $S_{Amplifier}$ represents the amplification factor used in the measurement, ADC_{pk-pk} is the distance between two neighbouring peaks, M_{ADC} is provided by the ADC manufacturer, and $e = 1.6\text{x}10^{-19} C$ is the electron charge. The gain has been measured applying different bias voltages to the CPTA device, and using and amplification factor of 20. The results are presented in Fig. 6, and Tab. 5. In the accessed range of bias voltages, the gain dependence is observed to be approximately linear. Deviation from linearity could be explained by systematical effects in the measurement setup.

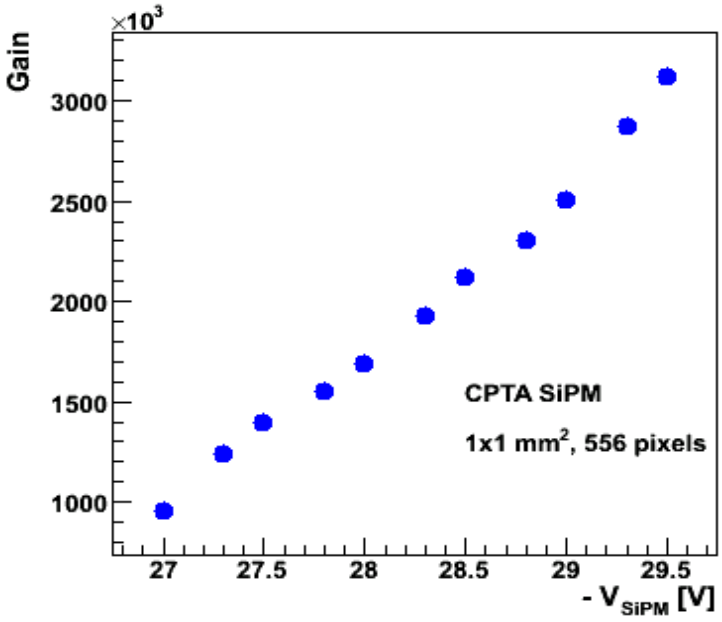

Fig. 6.: Gain dependence of CPTA SiPM on the voltage values applied to the silicon photomultiplier.

INPUT	V_{SiPM} [V]	27.0	27.3	27.5	27.8	28.0	28.3	28.5	28.8	29.0	29.3	29.5
OUTPUT	ADC_{pk1}	119	122	123	126	128	130	131	133	133	134	131
	ADC_{pk2}	134	142	145	151	155	161	165	170	173	180	181
	ADC_{pk1} - ADC_{pk2}	15	20	22	25	27	31	34	37	40	46	50
	G_{SiPM} [$\times 10^6$]	0.96	1.24	1.40	1.55	1.69	1.93	2.13	2.30	2.51	2.88	3.13

Table 5: Measurement of the gain dependence on the voltage values applied to CPTA SiPM. In this measurement the used amplification factor was 20, and the width of the signal pulse to switch the LED on was 22 ns.

5.3 HAMAMATSU MPPC Silicon Photomultipliers

Following the same experimental procedure used for CPTA SiPMs, the HAMAMATSU MPPCs silicon photomultipliers with size 1x1 mm^2 a nd 3x3 mm^2 have been investigated, directly coupled to the light source. The experimental setup is presented in Fig. 4. Differently from the CPTA SiPM case, here the LeCroy 1182 ADC module was used, with the gate width of 160 ns.

The single-pixels spectrum for the MPPC device of 1×1 mm² size and 400 pixels is shown in Fig.7 using an amplification factor of 20, and the peak values (in ADC units) are reported in Tab. 6. Measuring the peak to peak distance, the ADC values can be expressed in terms of effective firing pixels. Knowing the charge per ADC unit conversion factor (provided by the manufacturer) the gain was measured.

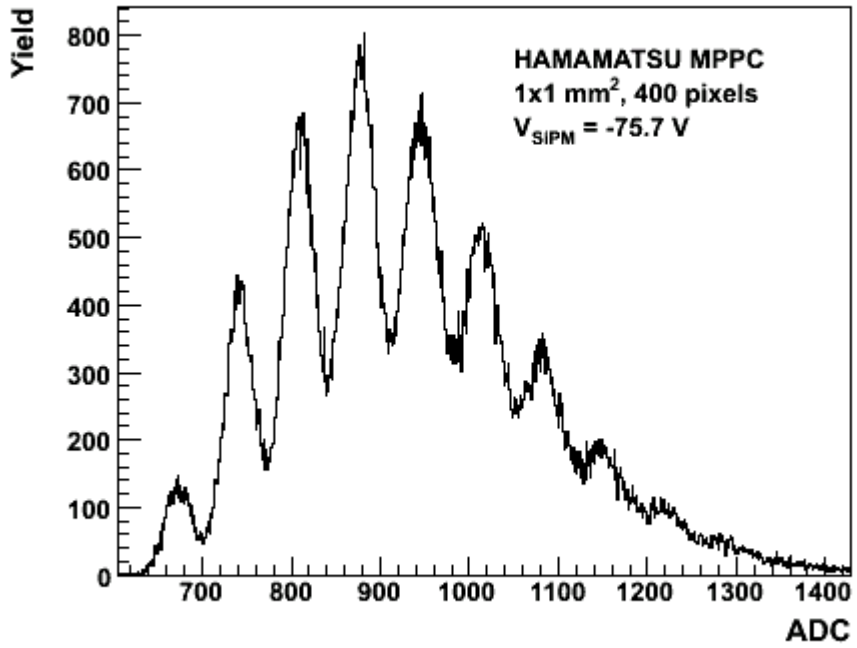

Fig. 7.: Single-pixel spectrum of HAMAMATSU MPPC 1×1 mm².

V_{SiPM} [V]	ADC_{pk2}	ADC_{pk3}	ADC_{pk4}	$\frac{ADC_{pk3}}{ADC_{pk2}}$	$\frac{ADC_{pk4}}{ADC_{pk3}}$	**ADC units per pixel**	G_{MPPC} $[x10^6]$
-75.7	752	820	887	68	67	67.5 (20X) 3.4 (1X)	0.52

Table 6: Measurement of single-pixel position values (in ADC units) in the energy spectrum of the HAMAMATSU MPPC of size 1×1 mm² and 400 pixels. Measuring the distance between two neighbouring peaks in ADC values, the ADC units can be then quantified expressed in number of photo-electron peaks.

The response of the device was measured for two different width values for the pulse used to switch the LED on. Increasing the pulse width should allow firing pixels to recover and to fire again within the same event (one LED flash). This feature is visible when comparing the results shown in Fig. 8 and Fig. 9, displaying the response of the photomultiplier for an LED pulse width of 22 and 40 ns. The corresponding measurement values are presented in Tab. 7 and Tab. 8.

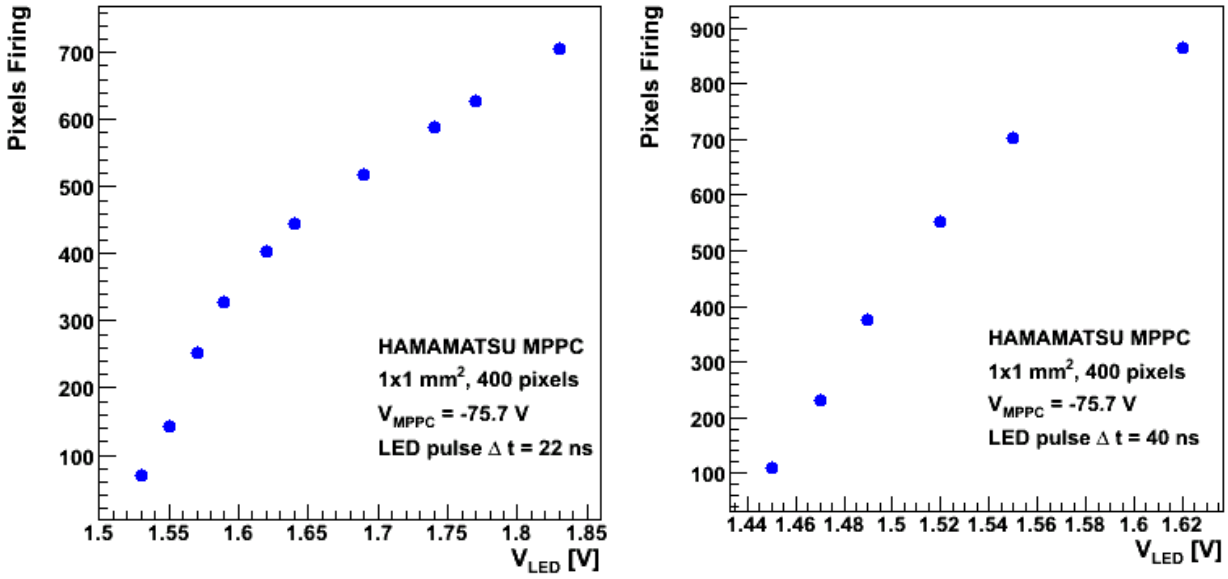

Fig. 8.: Response (in number of photo-electron pixels) of the HAMAMATSU MPPC 1x1 mm^2 to the input light intensity (presented in terms of the voltage value applied to the LED source) for an LED pulse width of 22 ns (left panel) and 40 ns (right panel).

INPUT	OUTPUT				
V_{LED} [V]	Signal [ADC]	Signal RMS	Pedestal [ADC]	Signal - Pedestal	Nr. of Pixels
1.53	880	28	649	231	68.5
1.55	1133	35	649	484	143.6
1.57	1497	34	649	848	251.6
1.59	1750	29	649	1101	326.7
1.62	2012	19	649	1363	404.4
1.64	2144	19	649	1495	443.6
1.69	2390	21	649	1741	516.6
1.74	2629	22	649	1980	587.5
1.77	2764	22	649	2115	627.6
1.83	3022	24	649	2373	704.1

Table 7: Measurement of the response HAMAMATSU MPPC 1×1 mm² (400 pixels) to the input signal amplitude for an LED pulse width of 22 ns.

INPUT	OUTPUT				
V_{LED} [V]	Signal [ADC]	Signal RMS	Pedestal [ADC]	Signal - Pedestal	Nr. of Pixels
1.45	1013	31	649	364	108.0
1.47	1431	36	649	782	232.0
1.49	1912	32	649	1263	374.8
1.52	2513	25	649	1864	553.1
1.55	3018	22	649	2369	703.0
1.62	3559	22	649	2910	863.5

Table 8: Measurement of the response HAMAMATSU MPPC 1×1 mm² (400 pixels) dependence to the input signal amplitude for an LED pulse width of 40 ns.

By changing the voltage bias to the silicon photomultiplier, and using an amplification factor of 20, the gain of the device was measured. Its linear dependence is shown in Fig. 9, and the values are reported in Tab. 9.

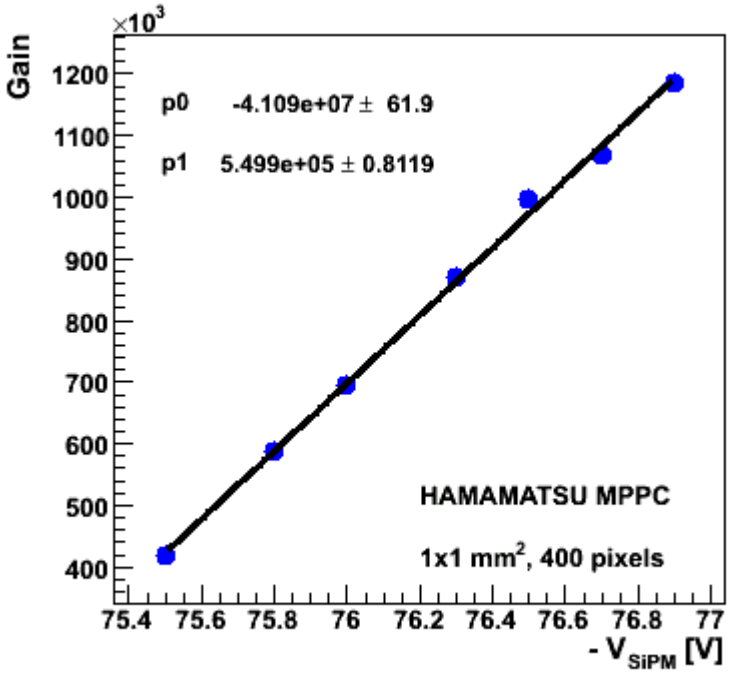

Fig. 9.: Gain dependence of HAMAMATSU MPPC 1×1 mm², 400 pixels.

INPUT	V_{SiPM} [V]	75.5	75.8	76.0	76.3	76.5	76.7	76.9
OUTPUT	ADC_{pk2}	744	757	765	780	785	792	794
	ADC_{pk3}	797	832	854	891	904	928	947
	ADC_{pk3} - ADC_{pk2}	53	75	89	111	129	136	153
	G_{MPPC} $[x10^6]$	0.42	0.59	0.70	0.87	1.01	1.07	1.19

Table 9: Measurement of the gain dependence on the voltage values applied to HAMAMATSU MPPC of size 1×1 mm², and 400 pixels. In this measurement the amplification factor used was 20, and the width of the signal pulse to switch the LED on was 22 ns.

A larger size MPPC (3×3 mm²) with 3600 pixels, was then investigated using the same experimental setup utilized for the MPPC 1×1 mm². For the readout, the LeCroy 1182 ADC module was used with the gate width of 160 ns. In this case, the single-pixel spectrum was measured with the amplification factor of 50. As usual, measuring the peak to peak distance, the ADC readout values can be expressed in terms of effective pixels firing, Tab. 10.

V_{SiPM} [V]	ADC_{pk2}	ADC_{pk3}	ADC_{pk4}	ADC_{pk3} – ADC_{pk2}	ADC_{pk4} – ADC_{pk3}	ADC units per pixel
-69.5	105	125	145	20	20	19.8 (50X) 0.4 (1X)

Table 10: Measurement of single-pixel position values (in ADC units) in the energy spectrum of the HAMAMATSU MPPC of size 3×3 mm² and with 3600 pixels. Measuring the distance between two neighbouring peaks in ADC values, the ADC units can be quantified expressed in number of photo-electron peaks.

Differently from the MPPC 1×1 mm² case, here the measurement of the linearity of the device was performed using a width pulse of 40 ns for switching the LED on. The much larger number of pixels in the device should decrease the effects of saturation. The device response to different amplitude values of the light source is shown in Fig. 10, and the values of the measurement are presented in Tab. 11.

The technology and size of the pixels for the analyzed MPPCs (1×1 mm² and 3×3 mm²) is the same, both types of photodetector should have the same gain, Fig. 9.

In the PET related measurements only the MPPC 3×3 mm² was used, its size matching with the crystal (3x3x15 mm^3) chosen as scintillator.

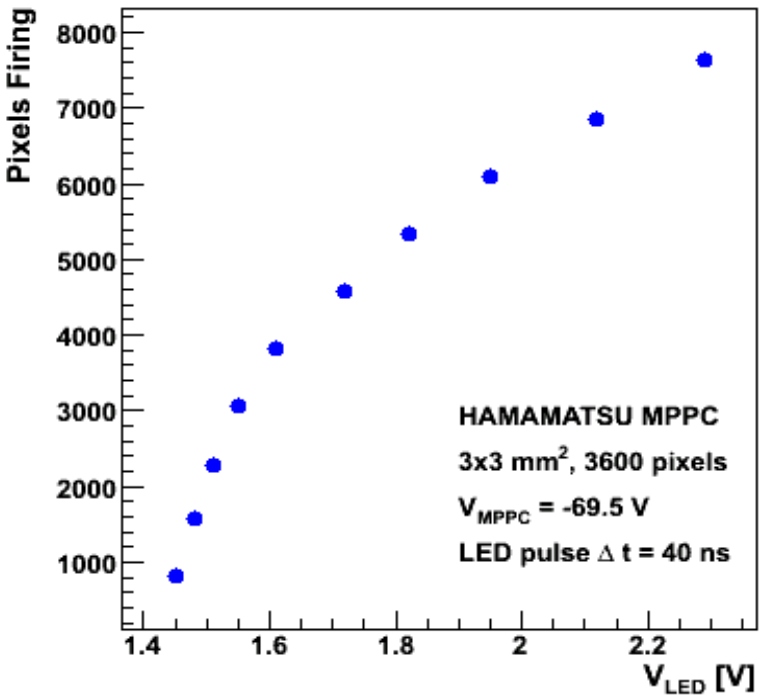

Fig. 10.: Response (in number of photo-electron pixels) of the HAMAMATSU MPPC of size 3x3 mm^2 with 3600 pixels, to the input light intensity (presented in terms of the voltage value applied to the LED source) for a LED pulse width of 40 ns.

INPUT	**OUTPUT**				
V_{LED} **[V]**	**Signal [ADC]**	**Signal RMS**	**Pedestal [ADC]**	**Signal - Pedestal**	**Nr. of Pixels**
1.45	412	9	91	321	807.6
1.48	719	9	91	628	1582.6
1.51	1007	9	91	916	2282.1
1.55	1312	5	91	1221	3075.6
1.61	1605	4	91	1504	3813.6
1.72	1913	3	91	1822	4589.4
1.82	2212	3	91	2121	5342.6
1.95	2514	3	91	2423	6103.3
2.12	2810	3	91	2719	6848.9
2.29	3116	6	91	3025	7619.6

Table 11: Response of the HAMAMATSU MPPC 3×3 mm² (3600 pixels) to the input signal amplitude for a LED pulse width of 40 ns.

5.4 Zecotek MAPD-3N Silicon Photomultipliers

The last investigated photodetector was the Zepotek MAPD-3N. The experimental apparatus was the same used for the MPPC silicon photomultipliers. Here, the LeCroy 1182 ADC module was used with a gate width of 120 ns.

For this photodetecor, due to the lower amplification factor of the device, it was not possible to resolve the photo-electron peak structure in the spectrum. Therefore, the gain could not be determined. Nevertheless, the MAPD-3N response to the input light amplitude could be still investigated, although without the possibility to quantify the response in term of number of effective firing pixels. The response measurement, applying a voltage bias of 89.4V to the device, is shown in Fig. 11, and the values are reported in Tab. 12. Within the (not quantified) systematic uncertainty of the measurement, the response appear reasonably linear, with no effects from saturation in the investigated range of input light. The effects from saturation could not be investigated, having reached the maximum voltage pulse amplitude provided by the pulse generator to switch the LED on. That generator can provide pulses up to 5 V.

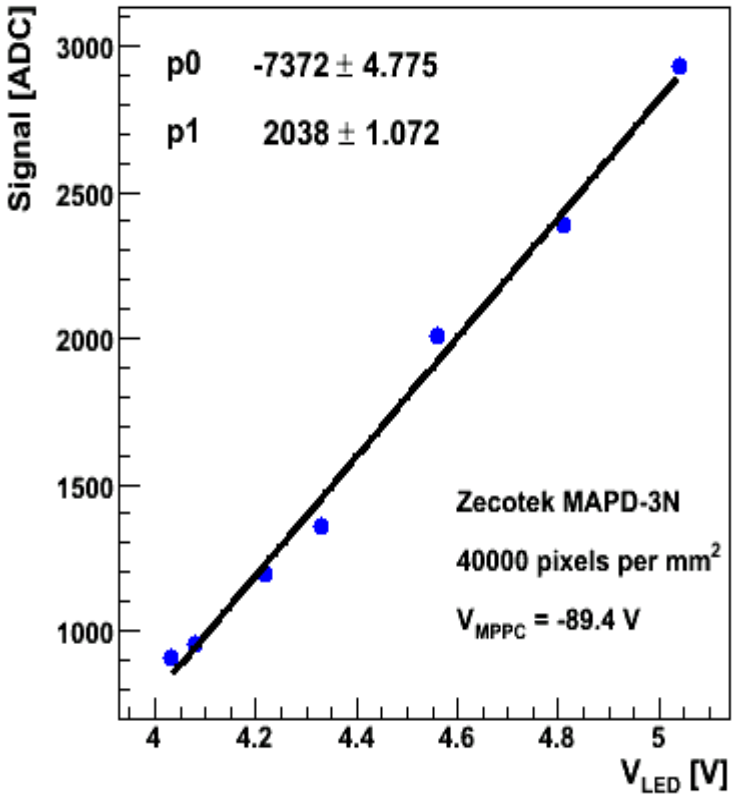

Fig. 11.: Response of the Zecotek MAPD-3N (in ADC units), to the input light intensity, presented in terms of the voltage value applied to the LED source.

INPUT	OUTPUT			
V_{LED} [V]	Signal [ADC]	Signal RMS	Pedestal [ADC]	Signal - Pedestal
4.03	1134	58	230	904
4.08	1186	58	230	956
4.22	1424	65	230	1194
4.33	1585	70	230	1355
4.56	2239	82	230	2009
4.81	2620	91	230	2390
5.04	3158	98	230	2928

Table 12: Measurement of the response to the input signal amplitude for the Zecotek MAPD-3N photodetector..

Although, for this photodetector the gain could not be measured, the response of the device to different voltage bias values could be investigated, while keeping the amplitude of the light source fixed. The measured dependence can be regarded as a gain measurement in arbitrary units (being unknown the amplitude of the incident light). This measurement is presented in Fig. 12, and the corresponding values are reported in Tab. 13.

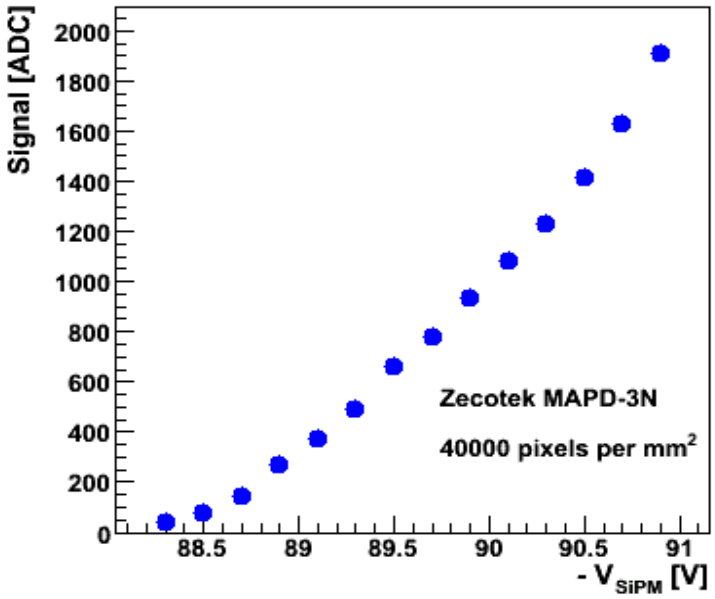

Fig. 12.: Measurement of the gain for the Zecotek MAPD-3N photodetector, in arbitrary units.

The dependence of the resolution (in percentage of ADC unit) on the voltage bias applied to the device could be calculated using the formula

Resolution [%] = RMS / (Signal-Pedestal) * 100.

The measured dependence is shown in Fig. 13 and Tab. 13.

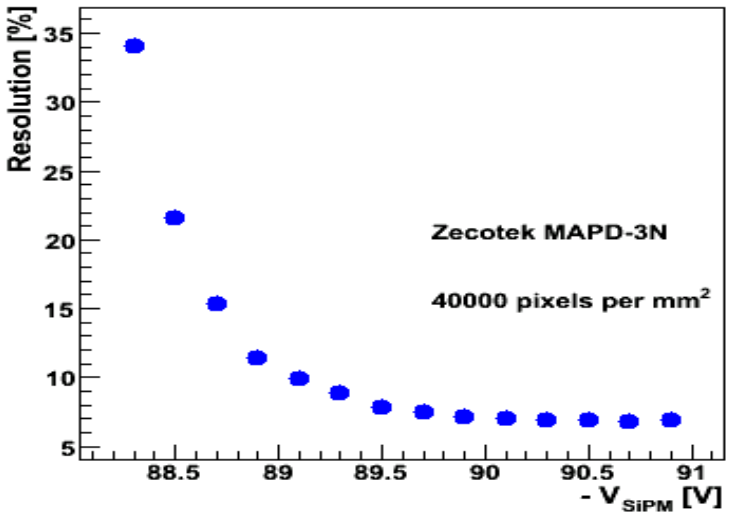

Fig. 13.: The energy resolution for the Zecotek MAPD-3N photodetector is presented as a function of the applied voltage bias, and in percentage of ADC counts.

INPUT	OUTPUT				
V_{SiPM} [V]	Signal [ADC]	RMS	Pedestal [ADC]	Signal - Pedestal	Resolution [%]
88.3	278	15	234	44	34.1
88.5	314	17	234	80	21.6
88.7	375	22	234	141	15.4
88.9	501	30	234	267	11.4
89.1	605	37	234	371	9.9
89.3	723	43	234	489	8.8
89.5	897	52	234	663	7.9
89.7	1010	58	234	776	7.5
89.9	1165	67	234	931	7.2
90.1	1314	76	234	1080	7.0
90.3	1467	85	234	1233	6.92
90.5	1646	97	234	1412	6.85
90.7	1863	111	234	1629	6.80
90.9	2142	131	234	1908	6.87

Table 13: Measurement of the MAPD-3N response and energy resolution (in percentage of ADC counts) to the input signal amplitude.

6. SiPM applications in PET

As mentioned in sec.4, an important application of silicon photomultipliers is in positron emission tomography. To realize this applicability the following measurement was performed using the experimental setup shown in Fig. 14.

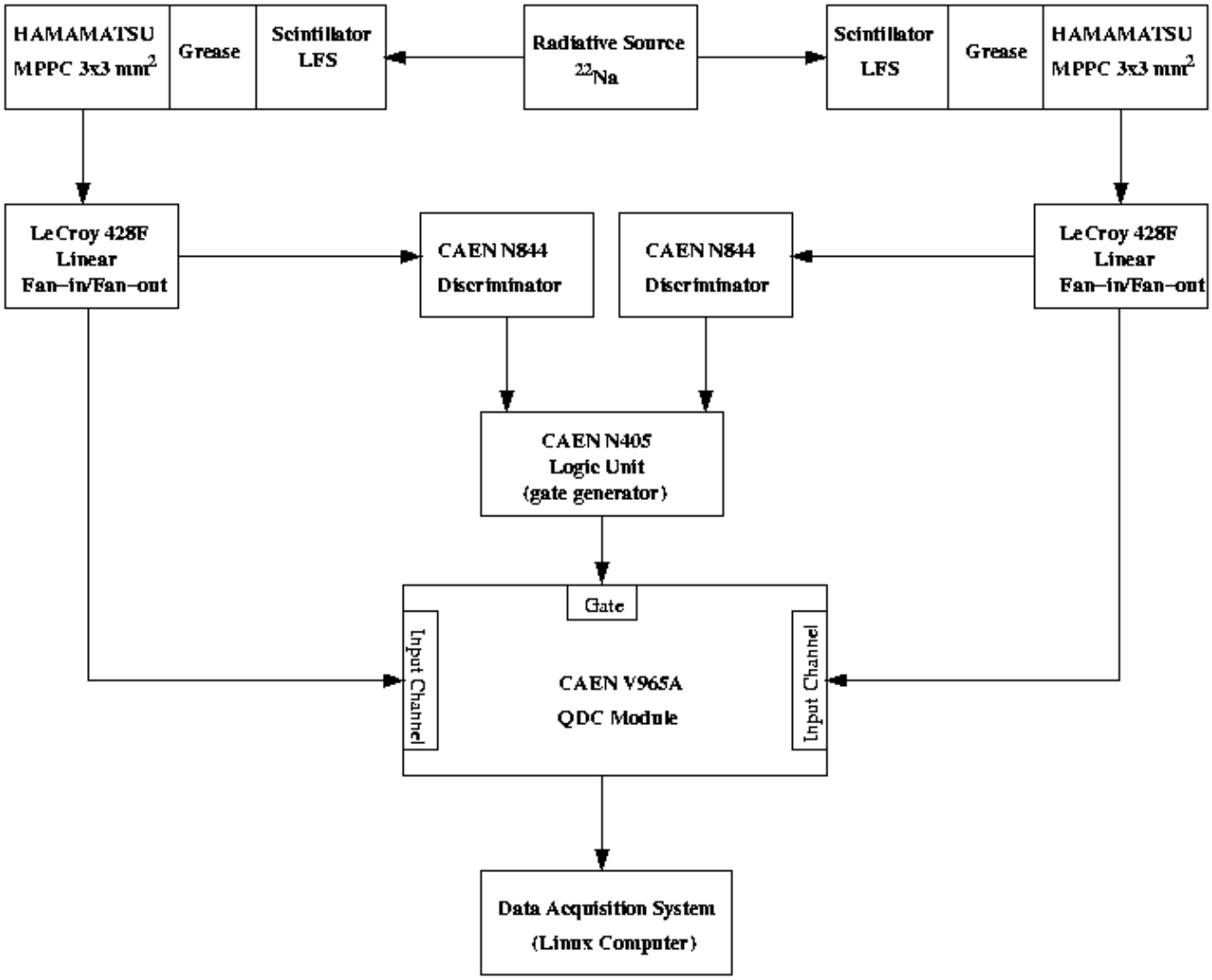

Fig. 14.: Experimental setup used for the PET application of silicon photomultipliers.

The radioactive source Na^{22} emits two photons with energy 511 keV in opposite directions. Each photon is detected by a photon detector. The photon device is made of one Lutetium Fine Silicate (LFS) crystal (with area 3×3 mm², and 15 mm length) coupled to one HAMAMATSU MPPC with area 3×3 mm² (3600 pixels) using Dow Corning's grease to improve the light collection. The signals from the crystals are individually read by the ADC module, once a coincidence event (above threshold) is observed (in the logic unit module). The result of the measurement is shown in Fig.14 and Fig. 15, separately for the two ADC channels.

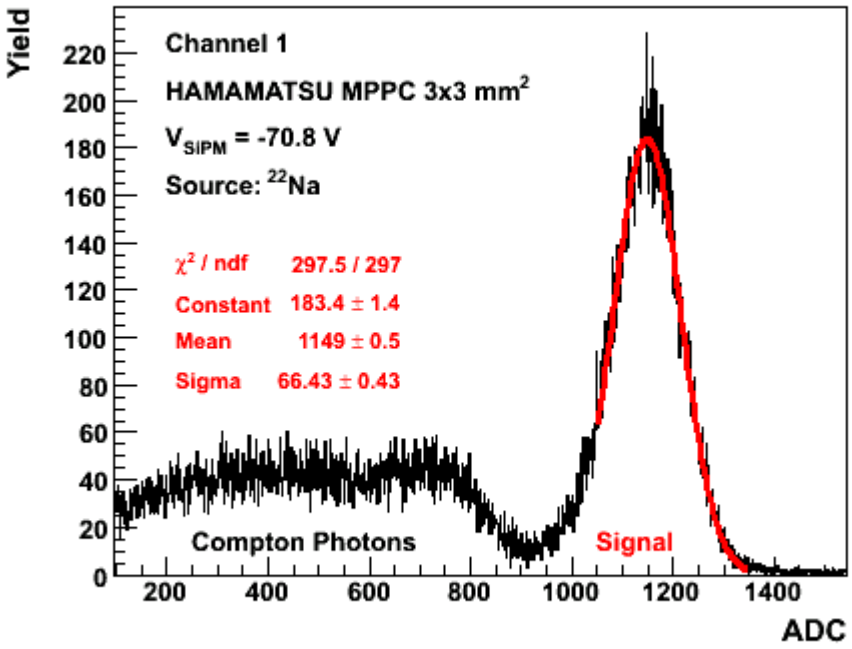

Fig. 15.: Photon energy spectrum recorded by channel one of the PET. Superimposed to the data is a gaussian fit to the photo-electron peak.

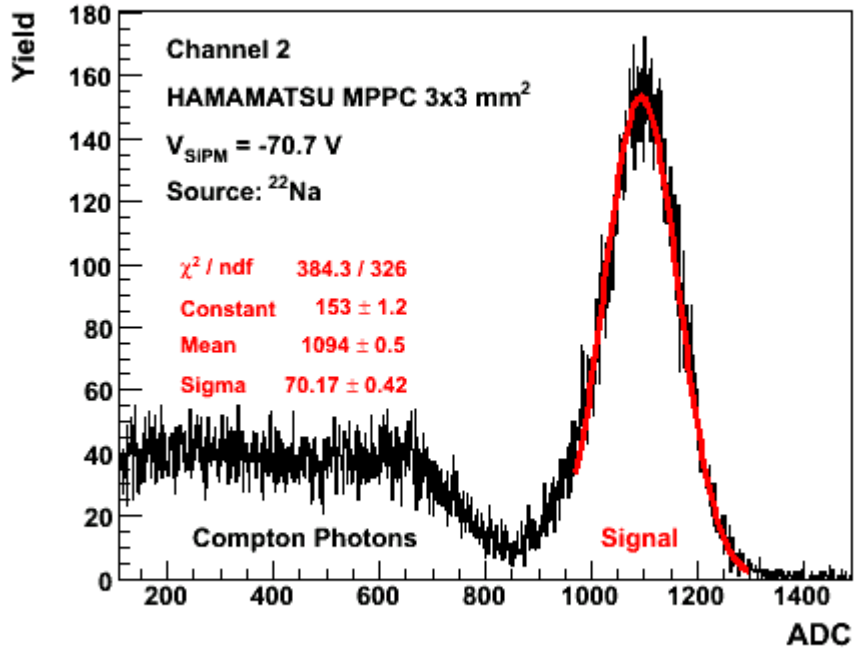

Fig. 16.: Photon energy spectrum recorded by channel two of the PET. Superimposed to the data is a gaussian fit to the photo-electron peak.

The energy resolution for the photo peak was calculated dividing the FWHM to the mean value of a gaussian fit to the data, and was measured to be around 12%. In the figures, the photo-electron peak (on the right side) is clearly well separated from the Compton photons background (left side). This gives a good possibility to use such photon detector (crystal + SiPM) for PET applications. The small size of the detector (3×3 mm²) should allow to measure the photon source location with reasonable precision.

6. Conclusions

In this work, different type of photodetectors were characterized. Saturation effects are visible in the response of the CPTA (integrated in a scintillating plate) SiPM and of the MPPCs of size 1×1 mm² and 3×3 mm². The saturation point is found to be around 1100 pixels for the CPTA SiPM. Due to the much larger number of pixels, the MAPD-3N device shows no clear effect from saturation in the range of light source amplitute accessible in the current experimental setup.

The quite low amplification factor of the MAPD-3N detector did not allow the determination of the device gain in absolute units. To disentangle the single-pixel structure in its spectrum an amplification factort larger that 50 (the maximum used in this work) is needed. Therefore, a direct comparison of its gain with the values obtained for the CPTA and Hamamatsu SiPMs (both linear in the investigated region of voltage bias values) cannot be done at this stage of the analysis. The measurements show the largest gain for the MPPC devices.

The feasibility of using silicon photomultipliers in PET applications was shown. The experimental setup for a PET prototype, developed at DESY, was used with the photodetector MPPC of size 3×3 mm² resulting in a clear separation of the signal from the Compton photon background, and in a relative energy resolution of approximately 12%. This gives a good possibility to use such photon detector in combination with the DESY PET prototype.

Acknowledgment

I would like to thank the organizing staff of the DESY Summer Student Program, especially Mrs. Schrader and Mr. Meyer. In spite of heavy duties in my university, I had a good time in Hamburg. Further thanks to my supervisors, Erika Garutti, Adel Terkulov, and Riccardo Fabbri for their nice guidance, great patience and tolerance. I also thank DESY for his achievements in HEP during its 50 years of activity, in particular for its attention to young students in natural sciences.

Bibliography

[1] J. Brau et al., International Linear Collider Report, ILC-REPORT-2007-001 (2007).
[2] P. Buzhan et al., Silicon Photomultiplier and its Possible Applications, Nucl. Inst. and Methods A504 (2003) 48.

[3] M. Yokoyama et al., Development of Multi-pixel Photon Counters (2006), arXiv:physics/0605241.
[4] W. R. Leo, Techniques for Nuclear and particle Physics Experiments, Springer-Verlag, 1994.
[5] D. W. Townsend, Physical Principles and Technology of Clinical PET Imaging, Ann. Acad. Med. Singapore, 33 (2004) 133.